



Received: 17 September 2010 – Accepted: 15 October 2010 – Published: 3 November 2010

Correspondence to: C. D. Nevison (nevison@colorado.edu)

Published by Copernicus Publications on behalf of the European Geosciences Union.

ACPD

10, 25803–25839, 2010

## Abiotic and biogeochemical signals

C. D. Nevison et al.

Title Page

Abstract

Introduction

Conclusions

References

Tables

Figures

◀

▶

◀

▶

Back

Close

Full Screen / Esc

Printer-friendly Version

Interactive Discussion



## Abstract

Seasonal cycles in the mixing ratios of tropospheric nitrous oxide ( $\text{N}_2\text{O}$ ) are derived by detrending long-term measurements made at sites across four global surface monitoring networks. These cycles are examined for physical and biogeochemical signals.

5 The detrended monthly data display large interannual variability, which at some sites challenges the concept of a “mean” seasonal cycle. The interannual variability in the seasonal cycle is not always correlated among networks that share common sites. In the Northern Hemisphere, correlations between detrended  $\text{N}_2\text{O}$  seasonal minima and polar winter lower stratospheric temperature provide compelling evidence for a strato-  
10 spheric influence, which varies in strength from year to year and can explain much of the interannual variability in the surface seasonal cycle. Even at sites where a strong, competing, regional  $\text{N}_2\text{O}$  source exists, such as from coastal upwelling at Trinidad Head, California, the stratospheric influence must be understood in order to interpret the biogeochemical signal in monthly mean data. In the Southern Hemisphere, de-  
15 trended surface  $\text{N}_2\text{O}$  monthly means are correlated with polar lower stratospheric temperature in months preceding the  $\text{N}_2\text{O}$  minimum, suggesting a coherent stratospheric influence in that hemisphere as well. A decomposition of the  $\text{N}_2\text{O}$  seasonal cycle in the extratropical Southern Hemisphere suggests that ventilation of deep ocean water (microbially enriched in  $\text{N}_2\text{O}$ ) and the stratospheric influx make similar contributions in  
20 phasing, and may be difficult to disentangle. In addition, there is a thermal signal in  $\text{N}_2\text{O}$  due to seasonal ingassing and outgassing of cooling and warming surface waters that is out of phase and thus competes with the stratospheric and ventilation signals. All the seasonal signals discussed above are subtle and are generally better quantified in high-frequency in situ data than in data from weekly flask samples, especially in the  
25 Northern Hemisphere. The importance of abiotic influences (thermal, stratospheric influx, and tropospheric transport) on  $\text{N}_2\text{O}$  seasonal cycles suggests that, at many sites, surface  $\text{N}_2\text{O}$  mixing ratio data by themselves are unlikely to provide information about seasonality in surface sources (e.g., for atmospheric inversions), but may be more

### Abiotic and biogeochemical signals

C. D. Nevison et al.

Title Page

Abstract

Introduction

Conclusions

References

Tables

Figures



Back

Close

Full Screen / Esc

Printer-friendly Version

Interactive Discussion



powerful if combined with complementary data such as CFC-12 mixing ratios or N<sub>2</sub>O isotopes.

## 1 Introduction

Nitrous oxide (N<sub>2</sub>O) is an important greenhouse gas with a global warming potential about 300 times that of CO<sub>2</sub> (Forster et al., 2007). It is the major source of NO to the stratosphere and, with the decline of chlorofluorocarbons (CFCs) in the atmosphere, is the dominant ozone-depleting substance emitted in the 21st Century (Ravishankara et al., 2009). The atmospheric N<sub>2</sub>O concentration has risen from about ~270 ppb preindustrially to ~320 ppb today (MacFarling-Meure et al., 2006), where the units of ppb (parts per billion) are used as a convenient shorthand for mole fraction mixing ratios of nanomoles of N<sub>2</sub>O per mole of dry air. Some of the best information about the global budget of atmospheric N<sub>2</sub>O has been derived from direct atmospheric monitoring, which has allowed the detection of long-term concentration trends and hence the inference of the relative strength of natural versus anthropogenic sources (Weiss et al., 1981; Prinn et al., 2000; Hirsch et al., 2006). Natural microbial production is known to account for about 2/3 of N<sub>2</sub>O emissions, but partitioning of this production between soils and oceans is uncertain. Anthropogenic sources are primarily associated with agriculture, either directly (e.g., emissions from fertilized fields) or indirectly (e.g., emissions from estuaries polluted with fertilizer runoff) (Forster et al., 2007). It is unclear to what extent anthropogenic emissions can be mitigated in the future, given the need to feed the expanding human population (Kroeze et al., 1999; Mosier et al., 2000).

While large uncertainties remain in bottom-up efforts to quantify N<sub>2</sub>O sources, the precision of direct atmospheric N<sub>2</sub>O measurements has improved to the point where small-amplitude seasonal cycles (currently in the range of 0.1–0.3% of the background mixing ratio), superimposed on the more dramatic secular increase, can be detected (Nevison et al., 2004, 2007; Jiang et al., 2007). However, recent top-down

### Abiotic and biogeochemical signals

C. D. Nevison et al.

Title Page

Abstract

Introduction

Conclusions

References

Tables

Figures



Back

Close

Full Screen / Esc

Printer-friendly Version

Interactive Discussion



approaches (i.e., atmospheric inversions) have not attempted to resolve seasonality in  $\text{N}_2\text{O}$  sources, in large part due to uncertainties over the influence of the flux of  $\text{N}_2\text{O}$ -depleted air from the stratosphere on tropospheric abundances (Hirsch et al., 2006; Huang et al., 2008).

In this paper, we examine the causes of seasonal variability in atmospheric  $\text{N}_2\text{O}$  at a range of surface monitoring sites, using data from four different monitoring networks. Our primary goal is to assess whether seasonal variations in the  $\text{N}_2\text{O}$  mixing ratio are dominated by biogeochemical signals or by abiotic factors that provide little direct information about surface sources. We focus in particular on sites in the Southern Hemisphere, where the impact of the stratospheric influx of  $\text{N}_2\text{O}$ -depleted air is most uncertain, sites where more than one monitoring network is present, and sites that have contemporaneous CFC-12 measurements. CFC-12 has a similar lifetime and stratospheric sink to  $\text{N}_2\text{O}$ , but few remaining surface sources. We therefore assume that correlated variability in CFC-12 and  $\text{N}_2\text{O}$  primarily reflects transport and stratospheric influences (Nevison et al., 2004, 2007), although this may not always be true, e.g., for air masses coming off the land in developing countries with active sources of both gases.

## 2 Methods

### 2.1 $\text{N}_2\text{O}$ and CFC-12 data

The longest records of atmospheric  $\text{N}_2\text{O}$  are available from the Advanced Global Atmospheric Gases Experiment (AGAGE) and its predecessors (Prinn et al., 2000) and the NOAA Halocarbons and other Atmospheric Trace Species (HATS) (Thompson et al., 2004) networks. Both AGAGE and NOAA/HATS also monitor CFC-12. While both networks began in the late 1970s, the instrumentation has evolved over the years and the high precision data needed to reliably detect seasonal cycles in  $\text{N}_2\text{O}$  are available from the early to mid 1990s for AGAGE and from the late 1990s for NOAA/HATS. The

## Abiotic and biogeochemical signals

C. D. Nevison et al.

Title Page

Abstract

Introduction

Conclusions

References

Tables

Figures

◀

▶

◀

▶

Back

Close

Full Screen / Esc

Printer-friendly Version

Interactive Discussion



**Abiotic and  
biogeochemical  
signals**

C. D. Nevison et al.

Title Page

Abstract

Introduction

Conclusions

References

Tables

Figures

◀

▶

◀

▶

Back

Close

Full Screen / Esc

Printer-friendly Version

Interactive Discussion



networks include 5 to 6 baseline stations each, making frequent measurements (every ~40 min) using in situ gas chromatography. The relative precision of the individual AGAGE measurements is about 0.03% (0.1 ppb) for N<sub>2</sub>O and slightly less precise for CFC-12. All AGAGE data are measured on the SIO 2005 calibration scale. Monthly mean values are estimated based on the order of 10<sup>3</sup> measurements, with local pollution events removed. Pollution events are defined based on a 2 sigma deviation from the mean. The NOAA/HATS in situ data are measured using the Chromatograph for Atmospheric Trace Species instruments, abbreviated as CATS. All NOAA data are measured on the NOAA 2006 calibration scale for N<sub>2</sub>O and the NOAA 2008 scale for CFC-12.

In addition to the in situ data, the NOAA Carbon Cycle Greenhouse Gases (CCGG) group and the Commonwealth Scientific and Industrial Research Organization (CSIRO) of Australia maintain flask networks, in which duplicate samples are collected every ~1 to 2 weeks and shipped for analysis on a central gas chromatograph. The CSIRO sites are located primarily in the Southern Hemisphere and date from the early 1990s, while NOAA/CCGG began monitoring N<sub>2</sub>O at ~60 widely distributed flask sampling sites in 1997. The reproducibility of NOAA/CCGG N<sub>2</sub>O measurements, based on the mean of absolute values of differences from flask pairs, is 0.4 ppb. The raw measurement precision for the CSIRO flask N<sub>2</sub>O data, which are measured on the CSIRO calibration scale, is estimated as +/-0.3 ppb (Francey et al., 2003). Neither NOAA/CCGG nor CSIRO provides concurrent CFC-12 measurements, however the NOAA/HATS group measures CFC-12 at a subset of the NOAA/CCGG observing sites. Flask and in situ CFC-12 data, if available, are combined in a product referred to as “NOAA/HATS Combined”. Table 1 lists the names, code letters, networks, and locations of the sites from which data have been analyzed in this paper.

## 2.2 Mean seasonal cycles and interannual variability

The N<sub>2</sub>O monthly mean data were detrended by subtracting a 12-month running mean, centered on the month in question, to remove the secular trend and other low fre-

quency variability. The remaining high frequency residuals were sorted by month and regressed against several proxies, described below, in an effort to identify causes of interannual variability in the N<sub>2</sub>O seasonal cycle. A 3rd order polynomial fit was found to adequately represent the secular trend in data at sites without gaps in the monthly mean record, and thus was used as a placeholder in the 12-month centered running mean at sites with gaps. A “mean” seasonal cycle was calculated by taking the average of the detrended data for all Januaries, Februaries, etc.

### 2.3 Proxies and indices

The detrended monthly means, sorted by month, were regressed against mean polar (60°–90°) lower stratospheric temperature at 100 hPa in winter/spring (January–March in the Northern Hemisphere, September–November in the Southern Hemisphere) from NCEP reanalyses (P. Newman, personal communication), a proxy for the strength of downwelling of N<sub>2</sub>O- and CFC-depleted air into the lower stratosphere (Nevison et al., 2007). For the Southern Hemisphere regressions, temperature data from the previous year, relative to that of the N<sub>2</sub>O data, were used in the regressions for January–August, since the effect of the austral winter stratospheric downwelling was not expected to be felt in the troposphere until September at earliest. In the Southern Hemisphere, regressions also were performed between the detrended N<sub>2</sub>O data and the polar vortex break-up date, calculated from the method used in Nash et al. (1996) from NOAA/DOE Reanalysis-2 data at 450 K (Eric Nash, personal communication). For the Trinidad Head, California site, the N<sub>2</sub>O monthly anomalies were regressed against the NOAA Pacific Fisheries Environmental Laboratory (PFEL) coastal upwelling index (<http://www.pfeg.noaa.gov/products>), which is compiled for every 3 degrees of latitude along the Pacific Northwest coastline. For all regressions of detrended N<sub>2</sub>O monthly means against the proxies described above, the statistical significance of the monthly correlation coefficients was assessed by comparing the calculated *R* values to critical *R* values determined from a t-table as a function of *N*–2 degrees of freedom (see Box 15.3 of Sokal and Rohlf, 1981).

## Abiotic and biogeochemical signals

C. D. Nevison et al.

Title Page

Abstract

Introduction

Conclusions

References

Tables

Figures

◀

▶

◀

▶

Back

Close

Full Screen / Esc

Printer-friendly Version

Interactive Discussion



## 2.4 Thermal signals

Atmospheric signals due to seasonal ingassing and outgassing associated with the changing solubility of cooling and warming ocean waters were estimated for N<sub>2</sub>O and CFC-12. These were calculated from a simulation of the MATCH atmospheric transport model (Mahowald et al., 1997) forced with a mean annual cycle of thermal O<sub>2</sub> fluxes calculated based on NCEP heat fluxes (Kalnay et al., 1996) and the formula of Jin et al. (2007). The thermal cycles of N<sub>2</sub>O and CFC-12 were estimated from the modeled O<sub>2</sub> thermal cycles by scaling by the ratio of the temperature derivative of the respective solubility coefficients (Nevison et al., 2005).

## 3 Results and discussion

### 3.1 Mean annual cycle

The seasonal cycles in N<sub>2</sub>O are small, with mean amplitudes ranging from about 0.3 to 0.9 ppb (Table 1), which amounts to only ~0.1 to 0.3% of the mean tropospheric mixing ratio of 320 ppb. The late summer minima observed in surface N<sub>2</sub>O at MHD, BRW (Figs. 1a, S1) and many other Northern Hemisphere sites are also seen in CFC-12 data (Nevison et al., 2004, 2007; Jiang et al., 2007). These minima are consistent with a stratospheric signal in which air depleted in both N<sub>2</sub>O and CFC-12 descends from the middle and upper stratosphere during winter due to the Brewer-Dobson circulation, undergoes stratosphere-troposphere exchange (STE), and propagates down to the lower troposphere with a delay of about 3 months (Holton et al., 1995; Nevison et al., 2007; Liang et al., 2008, 2009). Model studies indicate that STE of this N<sub>2</sub>O- and CFC-depleted air peaks in spring, with maximum injection in the 50°–60° N latitude band, although the exact location of maximum injection is likely a model-specific result and may vary seasonally with the position of the jet stream (Gettelman and Sobel, 2000; Liang et al., 2008, 2009).

## Abiotic and biogeochemical signals

C. D. Nevison et al.

Title Page

Abstract

Introduction

Conclusions

References

Tables

Figures

⏪

⏩

◀

▶

Back

Close

Full Screen / Esc

Printer-friendly Version

Interactive Discussion



**Abiotic and  
biogeochemical  
signals**

C. D. Nevison et al.

Title Page

Abstract

Introduction

Conclusions

References

Tables

Figures

◀

▶

◀

▶

Back

Close

Full Screen / Esc

Printer-friendly Version

Interactive Discussion



The late summer minima also reflect tropospheric transport mechanisms, e.g., summer vs. winter differences in convection and boundary layer thickness. Nevison et al. (2007) ran a chemical transport model without stratospheric sinks and still obtained late summer minima in  $N_2O$  and CFC-12 at some northern sites, due to seasonal variations in tropospheric transport and circulation. Liang et al. (2008) ran CFC-12 in an AGCM and found that the surface seasonal cycle was dominated by the stratospheric influence after the mid-1990s, but with an increasing contribution from tropospheric transport as one moved from mid to high latitudes. However, in the Southern Hemisphere, neither Nevison et al. nor Liang et al. were able to explain the observed fall minima of the  $N_2O$  (Figs. 1b, S2) and CFC-12 seasonal cycles based on surface sources and tropospheric transport alone.

A third abiotic influence on atmospheric  $N_2O$  data is the thermal signal due to changing solubility in warming and cooling surface ocean waters. The thermal signal is maximum in late summer in both hemispheres. It tends to oppose the observed seasonal cycle at most sites, although not at THD (Fig. 2), and thus cannot by itself explain the observed cycle.

### 3.2 Differences among monitoring networks

$N_2O$  data display considerable interannual variability, such that the concept of a “mean” seasonal cycle may not be very meaningful at some sites (Fig. 2). In addition, different monitoring networks that share common sites sometimes observe seasonal cycles that differ substantially in both shape and amplitude (Figs. 1a,b, S1, S2, Table 1). Some of the variability among networks may reflect local meteorology at the time of sampling or data filtering. To evaluate this possibility, we examined, for each month of the seasonal cycle, whether the detrended  $N_2O$  monthly means from different networks that share a common site showed correlated interannual variability. At Mace Head, which is sampled by both the in situ AGAGE network and the NOAA/CCGG flask network, the detrended, pollution-filtered AGAGE data (Fig. 1a) are not significantly correlated to the NOAA/CCGG data for any month. In contrast, at Cape Grim, which is sampled

by AGAGE, NOAA/CCGG and the CSIRO flask network (Fig. 1b), the detrended N<sub>2</sub>O monthly means are significantly correlated among the three networks, although only in ~March–May around the time of the seasonal minimum, with *R* values around 0.7. At Barrow, Alaska, the detrended N<sub>2</sub>O monthly means are not significantly correlated between NOAA/CCGG and in situ CATS data (Fig. S1). At the South Pole, the detrended N<sub>2</sub>O data are weakly correlated around the time of the May seasonal minimum among the NOAA/CATS, NOAA/CCGG and CSIRO networks, although with *R* values only around 0.5 (Fig. S2).

The lack of correlation in detrended N<sub>2</sub>O data between NOAA/CCGG and the AGAGE and NOAA/CATS networks at Mace Head and Barrow, respectively, could reflect limitations specific to NOAA/CCGG data. Alternatively, it could reflect the fact that interannual variability in the N<sub>2</sub>O seasonal cycle at northern sites is more strongly influenced by local conditions, including meteorology and pollution events, and data filtering artifacts than at southern sites. At MHD, about 20% of the in situ AGAGE measurements are tagged as pollution events compare to only 5% at CGO. When AGAGE data are subsampled at MHD at the time of NOAA/CCGG flask collection, the subsampled dataset picks up a number of somewhat erratic features that show up in the NOAA/CCGG data, but that are smoothed out or tagged as pollution events in the full AGAGE dataset (Fig. 3a,b). At CGO, subsampling of the AGAGE data at the time of NOAA/CCGG or CSIRO flask collection can explain some of the differences between the full AGAGE dataset and the two flask networks (Fig. 4). However, it does not appear to be the only factor governing the discrepancies among the networks (Fig. 4b,c). In general, detecting subtle seasonal and interannual signals in N<sub>2</sub>O data is more difficult for a flask network sampling every 1–2 weeks, with an average flask pair agreement of 0.4 ppb (in the case of NOAA/CCGG), than for an in situ network with a high-frequency measurement record.

**Abiotic and  
biogeochemical  
signals**

C. D. Nevison et al.

Title Page

Abstract

Introduction

Conclusions

References

Tables

Figures

◀

▶

◀

▶

Back

Close

Full Screen / Esc

Printer-friendly Version

Interactive Discussion



### 3.3 Interannual variations in the seasonal cycle

#### 3.3.1 Northern Hemisphere

In an effort to understand the causes of N<sub>2</sub>O seasonality, we compared interannual variability in the seasonal cycle to several proxies that offer mechanistic insight. The first of these proxies was mean winter polar lower stratospheric temperature. Interannual variation in the strength of the Brewer-Dobson circulation affects the extent to which warm middle and upper stratospheric air, which is depleted in N<sub>2</sub>O and CFCs due to photolysis and oxidation, descends into the polar lower stratosphere, causing temperature to covary with N<sub>2</sub>O and CFC minimum anomalies. The N<sub>2</sub>O and CFC minima in turn propagate into the troposphere through stratosphere-troposphere exchange. We interpret correlations between polar winter lower stratospheric temperature and detrended tropospheric N<sub>2</sub>O or CFC seasonal minima as evidence of a stratospheric influence on the tropospheric seasonal cycle. However, we can not rule out the possibility that these correlations might arise if tropospheric N<sub>2</sub>O and CFC-12 variability is driven by weather anomalies, e.g., in convection over continents, that in turn correlate with stratospheric temperatures.

When the detrended AGAGE MHD N<sub>2</sub>O monthly means from Fig. 1a, sorted by month, are plotted against stratospheric temperature, statistically significant anticorrelations are found in July–September, the months surrounding the August minimum (Fig. 5). Deeper minima occur during warm years, consistent with the stratospheric influence hypothesized above. While the strongest *R* value occurs in August, a summary of the monthly results shows additional significant positive correlations with stratospheric temperature for the February-March data, near the time of the N<sub>2</sub>O maximum and before one would expect the stratospheric influence from the current year's Brewer-Dobson circulation to be felt in the troposphere (Fig. 6). These February-March correlations may be a function of our detrending methodology (using a centered, 12-month running mean). Atmospheric growth rate anomalies in N<sub>2</sub>O at MHD are themselves correlated to lower stratospheric temperature, with slower growth occurring in warm

## Abiotic and biogeochemical signals

C. D. Nevison et al.

Title Page

Abstract

Introduction

Conclusions

References

Tables

Figures



Back

Close

Full Screen / Esc

Printer-friendly Version

Interactive Discussion



years (Nevison et al., 2007), resulting in a flatter curve being subtracted from the raw monthly mean N<sub>2</sub>O data in warm years.

In addition to the AGAGE N<sub>2</sub>O correlations at MHD, Fig. 7 and Table 1 show significant correlations between mean winter polar lower stratospheric temperature and the detrended N<sub>2</sub>O seasonal minima at ALT and BRW for CSIRO and CATS data, respectively. At MHD, NOAA/CCGG detrended N<sub>2</sub>O minima show a weak, although not statistically significant, anticorrelation with stratospheric temperature (Fig. 7b). Figure 3b suggests that the difference between the AGAGE and NOAA/CCGG results at MHD may be a sampling issue, in which the relatively infrequent weekly NOAA/CCGG flask samples intersect with pollution influences and noise due to atmospheric variability in the N<sub>2</sub>O data to obscure subtle interannual signals. In support of this hypothesis, the AGAGE N<sub>2</sub>O data at MHD are themselves only weakly anticorrelated with stratospheric temperature when pollution-filtered monthly means are replaced with unfiltered data, with the *R* values for the detrended August monthly means dropping from 0.87 to 0.49.

At MHD and THD (AGAGE data), significant anticorrelations are observed between stratospheric temperature and detrended CFC-12 seasonal minima (Fig. 7e,f). At BRW, the detrended NOAA/CATS CFC-12 minima are correlated with stratospheric temperature, although the correlation is not as robust as for NOAA/CATS N<sub>2</sub>O. The NOAA/HATS combined in situ/flask CFC-12 minima at BRW are also weakly but significantly correlated with stratospheric temperature for time series beginning in the 1990s and extending through the present. At MHD, where the strongest correlations with stratospheric temperature are observed for both AGAGE N<sub>2</sub>O and CFC-12 minima, the regressions yield slopes (in ppb/K) with a ratio of about 0.7 (where CFC-12 has been normalized to N<sub>2</sub>O units by multiplying by  $[x(\text{N}_2\text{O})/\text{ppb}]/[x(\text{CFC-12})/\text{ppt}]$ ). The 0.7 ratio is notably similar to the Volk et al. (1996) slope of normalized N<sub>2</sub>O vs. CFC-12 data measured near the tropopause.

For the northern sites in Fig. 7, the strongest correlation with stratospheric temperature typically occurs during the month of the N<sub>2</sub>O or CFC-12 minimum (August or

## Abiotic and biogeochemical signals

C. D. Nevison et al.

Title Page

Abstract

Introduction

Conclusions

References

Tables

Figures

◀

▶

◀

▶

Back

Close

Full Screen / Esc

Printer-friendly Version

Interactive Discussion



September), although additional correlations in the months surrounding the minimum also occur in some cases. The correlation coefficients in Fig. 7 and Table 1 indicate that the interannual variability in the stratospheric signal can account for anywhere between ~75% (at MHD) and ~25% (at ALT) of the variability in the detrended minima. Noise in the data, biogeochemical sources and tropospheric transport variability, especially at high latitudes, may account for the remainder.

Trinidad Head, California is an interesting case in which the detrended CFC-12 monthly means are significantly anticorrelated to stratospheric temperature in August, but the detrended N<sub>2</sub>O monthly means are not (Fig. 8a,c). Since N<sub>2</sub>O data at THD are known to be influenced by ventilation of N<sub>2</sub>O-enriched deepwater during coastal upwelling events (Lueker et al., 2003), we performed additional regressions of THD detrended N<sub>2</sub>O data against the coastal upwelling index for the Pacific Northwest. Correlations of  $R=0.45$  to  $0.66$  were found in April–September (the upwelling season), with more positive N<sub>2</sub>O values occurring during years of strong upwelling (Fig. 8b). A multivariate regression of detrended N<sub>2</sub>O data against the upwelling index and stratospheric temperature improved these correlations to  $R=0.64$  to  $0.82$  for April–September (Fig. 8d). Statistically significant correlations were obtained from the multivariate regression using the coastal upwelling indices at 42° N, 45° N and 48° N (THD is at 40° N), with best results obtained for the 45° N index. The results at THD indicate that sites located near strong regional N<sub>2</sub>O sources are also substantially affected by the stratospheric influx and that the latter influence must be accounted for in order to best interpret the biogeochemical signal in monthly mean data.

### 3.3.2 Southern Hemisphere

In previous studies, the stratospheric influence on N<sub>2</sub>O and CFC-12 has been less clear in the Southern Hemisphere than in the Northern Hemisphere. Two atmospheric general circulation-chemical transport models, the Whole Atmosphere Community Climate Model (WACCM) and National Institute for Environmental Studies (NIES) model did not produce a stratospheric signal in N<sub>2</sub>O at surface sites in the Southern Hemisphere,

## Abiotic and biogeochemical signals

C. D. Nevison et al.

Title Page

Abstract

Introduction

Conclusions

References

Tables

Figures

◀

▶

◀

▶

Back

Close

Full Screen / Esc

Printer-friendly Version

Interactive Discussion



**Abiotic and  
biogeochemical  
signals**

C. D. Nevison et al.

Title Page

Abstract

Introduction

Conclusions

References

Tables

Figures

◀

▶

◀

▶

Back

Close

Full Screen / Esc

Printer-friendly Version

Interactive Discussion



although both models predicted a coherent signal in summer in the Northern Hemisphere (Nevison et al., 2004; Ishijima et al., 2010). In contrast, the GEOS CCM model predicted coherent cycles in CFC-12 with autumn minima (Liang et al., 2008), although the amplitudes were about 50% smaller than the corresponding Northern Hemisphere amplitudes. Isotopic evidence, i.e., seasonal enrichment in  $^{15}\text{N}\text{-N}_2\text{O}$  characteristic of stratospheric air, also provides support for a stratospheric signal in tropospheric  $\text{N}_2\text{O}$  at CGO (Park et al., 2008). In addition,  $\text{N}_2\text{O}$  and CFC-12 seasonal cycles and inter-annual growth rate anomalies at Cape Grim are generally well correlated, suggesting a common influence such as the stratospheric influx (Nevison et al., 2004, 2007).

Stratosphere-troposphere exchange (STE) in the Southern Hemisphere is not as well studied as in the Northern Hemisphere, although it is thought to be coupled to a Brewer-Dobson circulation with weaker, less strongly seasonal descent into the winter pole than in the Northern Hemisphere (Holton et al., 1995). The polar vortex is also more stable and persistent in the Southern Hemisphere, which traps  $\text{N}_2\text{O}$  and CFC-depleted air in the polar lower stratosphere longer and hinders exchange with mid-latitudes, where most STE occurs, until late spring or early summer (Nevison et al., 2007). The late polar vortex breakup, combined with a lower-stratosphere-to-surface propagation time of several months for the stratospheric signal, may explain the later minima (autumn vs. late summer) observed in the Southern vs. Northern Hemispheres (Nevison et al., 2004; Liang et al., 2008).

The detrended AGAGE  $\text{N}_2\text{O}$  monthly means at Cape Grim (Fig. 1b), sorted by month and plotted against austral polar lower stratospheric temperature from the previous winter-spring, show statistically significant anticorrelations in January–February, with more negative values occurring during warm years. By May–June, however, the detrended  $\text{N}_2\text{O}$  data become positively correlated to stratospheric temperature (Fig. 9). The summary plot of the CGO correlations with stratospheric temperature shows that, unlike in the Northern Hemisphere, the strongest anticorrelations are found several months before the seasonal minimum and that positive correlations are observed at and shortly after the month of the seasonal minimum. Similar correlation patterns with

stratospheric temperature are found for AGAGE CFC-12 (Fig. 10a).

In an effort to better understand these findings, and because the N<sub>2</sub>O minimum at CGO varies from February-June in individual years, most commonly occurring in April or May (Fig. 1b), we regressed the month of the AGAGE N<sub>2</sub>O minimum against polar vortex break-up date (ranging from mid-November to the end of December) and found that earlier minima tended to occur in years with early vortex breakup and later minima in years with late breakup ( $R=0.75$ ). However, warmer stratospheric temperatures are themselves significantly correlated with earlier vortex breakup ( $R=0.79$ ), such that the two indices provide more or less redundant, rather than independent, predictive capability for the detrended N<sub>2</sub>O monthly means.

The NOAA/CCGG flask data at CGO show correlation patterns with stratospheric temperature that are similar to those seen by AGAGE, although the correlations are statistically significant only in January (Fig. 10d, e). In addition, both the NOAA/CCGG and CSIRO flask networks show correlation patterns similar to those seen at CGO by AGAGE at many of their other extratropical southern sites (Fig. 11, Table 1). In most cases, the anticorrelations are strongest in the months preceding the N<sub>2</sub>O minimum, which typically occurs in May, with the exception of Macquarie Island, where the anticorrelation is strongest in May. At the South Pole, neither the CSIRO, CATS nor NOAA/CCGG networks shows statistically significant correlations between detrended N<sub>2</sub>O data and stratospheric temperature, although there is a hint of an anticorrelation in January–February in detrended CATS CFC-12 data (Table 1). Since STE of N<sub>2</sub>O-depleted air takes place mainly at midlatitudes (Ishijima et al., 2010), the South Pole site is more poorly situated than the other sites to detect the stratospheric signal.

The mixed results in Figs. 9–11 suggest that the stratospheric influx following polar vortex breakup does exert a coherent influence on the N<sub>2</sub>O seasonal cycle, but that this influence is weaker than in the Northern Hemisphere and noise in the data, due, e.g., to atmospheric variability, may confuse the signal, yielding inconsistent results among different monitoring sites. It is also possible that a regional biogeochemical source interferes with the stratospheric signal, as was shown for Trinidad Head, California

**Abiotic and  
biogeochemical  
signals**

C. D. Nevison et al.

Title Page

Abstract

Introduction

Conclusions

References

Tables

Figures



Back

Close

Full Screen / Esc

Printer-friendly Version

Interactive Discussion



(Figs. 2, 8).

Like Trinidad Head, monitoring sites in the Southern Ocean region are influenced by ventilation of oceanic, microbially-produced  $N_2O$ . This is especially true of sites situated in the heart of the Antarctic Circumpolar Current (Orsi et al., 1995), between  $\sim 50^\circ$ – $60^\circ$  S, where strong winds and upwelling lead to deep ventilation of  $N_2O$ -enriched subsurface waters. Nevison et al. (2005) hypothesized that the  $N_2O$  seasonal cycle at Cape Grim can be decomposed into comparable contributions from ocean ventilation, the stratospheric influx, and an abiotic thermal signal due to warming and cooling of surface waters (Fig. 12a). The stratospheric signal in Fig. 12a is estimated based on the observed, normalized CFC-12 cycle at CGO multiplied by a scaling factor which is uncertain, but which we assign a best guess value of 0.7 based on the discussion in Sect. 3.3.1.

Unlike THD, where the thermal signal is in phase with the summer upwelling  $N_2O$  source, ventilation of Southern Ocean waters occurs during the breakdown of the seasonal thermocline in fall and winter, and thus opposes the thermal signal. In Fig. 12b, the thermally-corrected  $N_2O$  cycle, i.e., subtracting the estimated thermal signal from the observed “mean” seasonal cycle, yields a cycle that closely resembles the observed CFC-12 cycle. (CFC-12 also experiences thermal ingassing and outgassing, but is 8 times less soluble than  $N_2O$ , such that the thermal correction has little impact on its cycle (Fig. 12b).) The ocean ventilation and stratospheric signals are roughly coincident, with the former a positive signal peaking in early fall and the latter a negative signal peaking in spring, making the two signals difficult to distinguish based on mixing ratio data alone. Indeed, the possibility that the thermally-corrected  $N_2O$  cycle in Fig. 12b is primarily or entirely due to the stratospheric influx with no influence from ocean ventilation cannot be ruled out, although this is inconsistent with evidence from atmospheric  $O_2/N_2$  data and ocean biogeochemistry models (Jin and Gruber, 2003; Nevison et al., 2005).

Even if the ocean ventilation signal is dwarfed by the stratospheric signal at CGO, which is located in a region of the Southern Ocean characterized by downwelling, it

**Abiotic and  
biogeochemical  
signals**

C. D. Nevison et al.

Title Page

Abstract

Introduction

Conclusions

References

Tables

Figures

◀

▶

◀

▶

Back

Close

Full Screen / Esc

Printer-friendly Version

Interactive Discussion



may be stronger at sites further poleward, in the upwelling region. We tested this hypothesis (following the example at THD) by regressing detrended  $N_2O$  monthly mean flask data at several Southern Hemisphere sites against a multivariate combination of stratospheric temperature and zonally-averaged NCEP wind speed or windstress curl at the latitude band of the site (Kalnay et al., 1996). Although no significant correlations were found, a more judicious or focused proxy for ocean ventilation, combined with an in situ  $N_2O$  record at a site within the upwelling region, arguably might yield better results. In addition, it may be necessary to account for interannual variability in the thermal signal, which directly competes with the ventilation signal.

## 4 Conclusions

Correlations between detrended tropospheric  $N_2O$  monthly mean data, sorted by month, and various interannually-varying proxies, including polar lower stratospheric temperature, polar vortex breakup date and coastal upwelling indices, are used to help identify the mechanisms that cause interannual variability in the  $N_2O$  seasonal cycle. In the months surrounding the  $N_2O$  seasonal minimum, the detrended  $N_2O$  data are significantly anti-correlated with winter polar lower stratospheric temperature at a number of Northern Hemisphere surface monitoring sites, with deeper minima occurring in warm years, providing strong empirical evidence that these seasonal cycles bear a stratospheric influence. At Trinidad Head, California, detrended  $N_2O$  monthly means in summer are weakly correlated to the index for coastal upwelling, which ventilates  $N_2O$ -enriched deepwater to the atmosphere, but more strongly correlated after the stratospheric influence is accounted for using a multivariate regression against both stratospheric temperature and the coastal upwelling index. Monitoring sites in the extratropical Southern Hemisphere, where the stratospheric influence on surface  $N_2O$  has been more difficult to establish in previous studies, also show anti-correlations between detrended  $N_2O$  monthly means and polar lower stratospheric temperature, although the anti-correlations generally are not centered on the month of the  $N_2O$

## Abiotic and biogeochemical signals

C. D. Nevison et al.

Title Page

Abstract

Introduction

Conclusions

References

Tables

Figures



Back

Close

Full Screen / Esc

Printer-friendly Version

Interactive Discussion



seasonal minimum as in the northern hemisphere, but rather are stronger in months preceding the minimum. Southern Ocean sites also are likely influenced by oceanic thermal and biological ventilation signals, but these influences are difficult to prove using the methodology of this study. N<sub>2</sub>O seasonal cycles can vary strongly year to year, making a “mean” cycle difficult to define at some sites, especially those subject to competing influences from various interannually-varying sources and sinks. Among networks that share a common site, interannual variability in detrended N<sub>2</sub>O monthly means is not necessarily well correlated, especially in the Northern Hemisphere. In part, this is a sampling issue, with weekly flask networks less able to detect subtle interannual signals and filter out noise due to atmospheric variability than more frequently sampled in situ networks. Due to the various abiotic influences on N<sub>2</sub>O seasonal cycles, including thermal oceanic in and outgassing, stratospheric influx, and tropospheric transport, sites that measure a complementary tracer, e.g., <sup>15</sup>N-N<sub>2</sub>O or CFC-12, that helps separate transport and stratospheric influences from soil and oceanic biogeochemical source signals are more likely to provide insight into seasonality in N<sub>2</sub>O sources.

**Supplementary material related to this article is available online at:**  
**[http://www.atmos-chem-phys-discuss.net/10/25803/2010/  
acpd-10-25803-2010-supplement.pdf](http://www.atmos-chem-phys-discuss.net/10/25803/2010/acpd-10-25803-2010-supplement.pdf)**

*Acknowledgement.* CDN acknowledges support from NASA grant NNX08AB48G and thanks Paul Newman and Eric Nash for stratospheric data and Qing Liang and Ralph Keeling for helpful comments. The authors are deeply grateful to the many people, from many organisations around the world, who have contributed to the production of the excellent N<sub>2</sub>O datasets that have made this study possible. These include the people who diligently collect flask air samples, those who analyze the flask samples, and those staff who maintain the optimal operation and calibration of in situ instruments at baseline sites.

**Abiotic and  
biogeochemical  
signals**

C. D. Nevison et al.

Title Page

Abstract

Introduction

Conclusions

References

Tables

Figures

◀

▶

◀

▶

Back

Close

Full Screen / Esc

Printer-friendly Version

Interactive Discussion



## References

- Forster, P., Ramaswamy, V., Artaxo, P., Bernsten, T., Betts, R., Fahey, D. W., Haywood, J., Lean, J., Lowe, D. C., Myhre, G., Nganga, J., Prinn, R., Raga, G., Schulz, M., and Van Dorland, R.: Changes in atmospheric constituents and in radiative forcing, in: Climate Change 2007: The Physical Science Basis. Contribution of Working Group I to the Fourth Assessment Report of the Intergovernmental Panel on Climate Change. Cambridge University Press Cambridge, UK and New York, NY, USA, 2007.
- Francey, R. J., Steele, L. P., Spencer, D. A., Langenfelds, R. L., Law, R. M., Krummel, P. B., Fraser, P. J., Etheridge, D. M., Derek, N., Coram, S. A., Cooper, L. N., Allison, C. E., Porter, L., and Baly, S.: The CSIRO (Australia) measurement of greenhouse gases in the global atmosphere, in: Baseline Atmospheric Program Australia 1999–2000, edited by: Tindale, N. W., Derek, N., and Fraser, P. J., Bureau of Meteorology and CSIRO Atmospheric Research, Melbourne, Australia, 42–53, 2003.
- Glatthor, N., et al.: Mixing processes during the Antarctic vortex split in September–October 2002 as inferred from source gas and ozone distributions from ENVISAT-MIPAS, *J. Atmos. Sci.*, 62(3), 787–800, 2005.
- Gettelman, A. and Sobel, A. H.: Direct diagnoses of stratosphere-troposphere exchange, *J. Atmos. Sci.*, 57(1), 3–16, 2000.
- Hirsch, A. I., Michalak, A. M., Bruhwiler, L. M., Peters, W., Dlugokencky, E. J., and Tans, P. P.: Inverse modeling estimates of the global nitrous oxide surface flux from 1998–2001, *Global Biogeochem. Cy.*, 20, GB1008, 2006.
- Holton, J. R., Haynes, P. H., McIntyre, M. E., Douglass, A. R., Rood, R. B., and Pfister, L.: Stratosphere-troposphere exchange, *Rev. Geophys.*, 33(4), 403–439, 1995.
- Huang, J., Golombek, A., Prinn, R., Weiss, R., Fraser, P., Simmonds, P., Dlugokencky, E. J., Hall, B., Elkins, J., Steele, P., Langenfelds, R., Krummel, P., Dutton, G., and Porter, L.: Estimation of regional emissions of nitrous oxide from 1997 to 2005 using multinet network measurements, a chemical transport model, and an inverse method, *J. Geophys. Res.* 113, D17313, doi:10.1029/2007JD009381, 2008.
- Ishijima, K., Nakazawa, T., Sugawara, S., Aoki, S., and Saeki, T.: Concentration variations of tropospheric nitrous oxide over Japan, *Geophys. Res. Lett.*, 28(1), 171–174, 2001.
- Ishijima, K., Patra, P. K., Takigawa, M., Machida, T., Matsueda, H., Sawa, Y., Steele, L. P., Krummel, P. B., Langenfelds, R. L., Aoki, S., and Nakazawa, T.: The stratospheric influence on

ACPD

10, 25803–25839, 2010

### Abiotic and biogeochemical signals

C. D. Nevison et al.

Title Page

Abstract

Introduction

Conclusions

References

Tables

Figures

◀

▶

◀

▶

Back

Close

Full Screen / Esc

Printer-friendly Version

Interactive Discussion



**Abiotic and  
biogeochemical  
signals**

C. D. Nevison et al.

Title Page

Abstract

Introduction

Conclusions

References

Tables

Figures

◀

▶

◀

▶

Back

Close

Full Screen / Esc

Printer-friendly Version

Interactive Discussion



the seasonal cycle of nitrous oxide in the troposphere as deduced from aircraft observations and model simulations, *J. Geophys. Res.*, doi:10.1029/2009JD013322, 2010.

Jiang, X., Ku, W. L., Shia, R.-L., Li, Q., Elkins, J. W., Prinn, R. G., and Yung, Y. L.: Seasonal cycle of N<sub>2</sub>O: analysis of data, *Global Biogeochem. Cy.*, 21, GB1006, 2007.

5 Jin, X. and Gruber, N.: Offsetting the radiative benefit of ocean iron fertilization by enhancing N<sub>2</sub>O emissions, *Geophys. Res. Lett.*, 30(24), 2249, 2003.

Jin, X., Najjar, R. G., Louanchi, F., and Doney, S. C.: A modeling study of the seasonal oxygen budget of the global ocean, *J. Geophys. Res.*, 112, C05017, doi:10.1029/2006JC003731, 2007.

10 Kalnay, E., Kanamitsu, M., Kistler, R., Collins, W., Deaven, D., et al.: The NMC/NCAR 40-year reanalysis project, *B. Am. Meteorol. Soc.*, 77, 437–471, 1996.

Kroeze, C., Mosier, A., and Bouwman, L.: Closing the global N<sub>2</sub>O budget: A retrospective analysis 1500–1994, *Global Biogeochem. Cy.*, 13, 1–8, 1999.

15 Liang, Q., Stolarski, R. S., Douglass, A. R., Newman, P. A., and Nielsen, J. E.: Evaluation of emissions and transport of CFCs using surface observations and their seasonal cycles and the GEOS CCM simulation with emissions-based forcing, *J. Geophys. Res.*, 113, doi:10.1029/2007JD009617, 2008.

20 Liang, Q., Douglass, A. R., Duncan, B. N., Stolarski, R. S., and Witte, J. C.: The governing processes and timescales of stratosphere-to-troposphere transport and its contribution to ozone in the Arctic troposphere, *Atmos. Chem. Phys.*, 9, 3011–3025, doi:10.5194/acp-9-3011-2009, 2009.

Liao, T., Camp, C. D., and Yung, Y. L.: The seasonal cycle of N<sub>2</sub>O, *Geophys. Res. Lett.*, 31, 17108, 2004.

25 Levin, I. P., Cias, P., Langenfelds, R., Schmidt, M., Ramonet, M., et al.: Three years of trace gas observations over the EuroSiberian domain derived from aircraft sampling – a concerted action, *Tellus*, 54B, 696–712, 2002.

Lueker, T. J., Walker, S. J., Vollmer, M. K., Keeling, R. F., Nevison, C. D., and Weiss, R. F.: Coastal upwelling air-sea fluxes revealed in atmospheric observations of O<sub>2</sub>/N<sub>2</sub>, CO<sub>2</sub> and N<sub>2</sub>O, *Geophys. Res. Lett.*, 30, 1292, 2003.

30 MacFarling Meure, C., Etheridge, D. M., Trudinger, C. M., Steele, L. P., Langenfelds, R. L., van Ommen, T., Smith, A., and Elkins, J. W.: Law Dome CO<sub>2</sub>, CH<sub>4</sub>, and N<sub>2</sub>O ice core records extended to 2000 years BP, *Geophys. Res. Lett.*, 33, L14810, 2006.

Mahowald, N. M., Rasch, P. J., Eaton, B. E., Whittlestone, S., and Prinn, R. G.: Transport of

## Abiotic and biogeochemical signals

C. D. Nevison et al.

Title Page

Abstract

Introduction

Conclusions

References

Tables

Figures

◀

▶

◀

▶

Back

Close

Full Screen / Esc

Printer-friendly Version

Interactive Discussion



radon-222 to the remote troposphere using the Model of Atmospheric Transport and Chemistry and assimilated winds from ECMWF and the National Center for Environmental Prediction/NCAR, *J. Geophys. Res.*, 102, 28139–28151, 1997.

Mosier, A. R., Duxbury, J. M., Freney, J. R., Heinemeyer, O., and Minami, K.: Assessing and mitigating N<sub>2</sub>O emissions from agricultural soils, *Climatic Change*, 40, 7–38, 2000.

Nevison, C. D., Kinnison, D. E., and Weiss, R. F.: Stratospheric Influence on the tropospheric seasonal cycles of nitrous oxide and chlorofluorocarbons, *Geophys. Res. Lett.*, 31(20), L20104, 2004.

Nevison, C. D., Keeling, R. F., Weiss, R. F., Popp, B. N., Jin, X., Fraser, P. J., Porter, L. W., and Hess, P. G.: Southern Ocean ventilation inferred from seasonal cycles of atmospheric N<sub>2</sub>O and O<sub>2</sub>/N<sub>2</sub> at Cape Grim, Tasmania, *Tellus*, 57B, 218–229, 2005.

Nevison, C. D., Mahowald, N. M., Weiss, R. F., and Prinn, R. G.: Interannual and seasonal variability in atmospheric N<sub>2</sub>O, *Global Biogeochem. Cy.*, 21, GB3017, 2007.

Orsi, A. H., Whitworth III, T., and Nowlin Jr., W. D.: On the meridional extent and fronts of the Antarctic Circumpolar Current, *Deep-Sea Res. Pt. I*, 42(5), 651–673, 1995.

Park, S., Boering, K. A., and Etheridge, D. M.: Trends, seasonal cycles, and interannual variability in the isotopic composition of nitrous oxide between 1940 and 2008, *Eos Trans.*, 89(53), Abstract A21A-0125, 2008.

Prinn, R. G., Weiss, R. F., Fraser, P. J., Simmonds, P. G., Cunnold, D. M., Alyea, F. N., O'Doherty, S., Salameh, P., Miller, B. R., Huang, J., Wang, R. H. J., Hartley, D. E., Harth, C., Steele, L. P., Sturrock, G., Midgley, P. M., and McCulloch, A.: A history of chemically and radiatively important gases in air deduced from ALE/GAGE/AGAGE, *J. Geophys. Res.*, 105(D14), 17751–17792, 2000.

Ravishankara, A. R., Daniel, J. S., and Portmann, R. W.: Nitrous oxide (N<sub>2</sub>O): The dominant ozone depleting substance emitted in the 21st century, *Science*, 326, 123–125, doi:10.1126/science.1176985, 2009.

Sokal, R. R. and Rohlf, F. J.: *Biometry*, W. H. Freeman, New York, USA, 859 pp., 1981.

Thompson, T. M., Elkins, J. W., Hall, B., et al.: Halocarbons and other atmospheric trace species, in: *Climate Diagnostics Laboratory Summary Report #27, 2002–2003*, edited by: Schnell, R. C., Buggle, A.-M., and Rossson, R. M., US Department of Commerce, National Oceanic and Atmospheric Administration, Boulder, Colorado, 2004.

Volk, C. M., Elkins, J. W., Fahey, D. W., Salawitch, R. J., Dutton, G. S., Gilligan, J. M., Proffitt, M. H., Loewenstein, M., Podolske, J. R., Minschwaner, K., Margitan, J. J., and

- Chan, K. R.: Quantifying transport between the tropical and mid-latitude lower stratosphere, *Science*, 272, 1763–1768, 1996.
- Weiss, R. F.: The temporal and spatial distribution of tropospheric nitrous oxide, *J. Geophys. Res.*, 86, 7185–7195, 1981.

---

**Abiotic and  
biogeochemical  
signals**

C. D. Nevison et al.

---

Title Page

Abstract

Introduction

Conclusions

References

Tables

Figures



Back

Close

Full Screen / Esc

Printer-friendly Version

Interactive Discussion



**Table 1.** Correlations between N<sub>2</sub>O seasonal minimum anomalies and mean polar (60°–90°) lower stratospheric (at 100 hPa) temperature for January–March (Northern Hemisphere) or September–November (Southern Hemisphere). Bold type in final column indicates statistically significant correlations ( $p \leq 0.05$ ).

Site	Name	Latitude	Longitude	Network <sup>a</sup>	Species	Starting date	Mean seasonal cycle		Correlation with stratospheric temperature		
							Month of minimum	Amplitude (ppb)	Month of best anti-correlation	Slope ppb K <sup>-1</sup>	<i>R</i>
ALT	Alert, Greenland	82.4	-62.5	N/CCGG	N <sub>2</sub> O	Jul 97	Sep	0.69	Nov	-0.070	<b>0.79</b>
ALT				CSIRO	N <sub>2</sub> O	Jul 92	Sep	0.81	Oct	-0.032	<b>0.64</b>
BRW	Barrow, Alaska	71.3	-156.5	N/CCGG	N <sub>2</sub> O	Jan 98	Aug	0.87	Sep	-0.040	<b>0.62</b>
BRW				N/CATS	N <sub>2</sub> O	Jun 98	Aug	0.93	Aug	-0.043	<b>0.67</b>
BRW				N/CATS	CFC-12	Jun 98	Sep	0.88 <sup>b</sup>	Sep	-0.062 <sup>b</sup>	<b>0.66</b>
BRW				N/HATS combined	CFC-12	Jan 90	Sep	1.1 <sup>b</sup>	Sep	-0.044 <sup>b</sup>	<b>0.46</b>
MHD	Mace Head, Ireland	53.3	-9.9	AGAGE	N <sub>2</sub> O	Nov 94	Aug	0.66	Aug	-0.032	<b>0.87</b>
MHD				AGAGE	CFC-12	Mar 94	Aug	0.89 <sup>b</sup>	Aug	-0.045 <sup>b</sup>	<b>0.92</b>
MHD				N/CCGG	N <sub>2</sub> O	Jan 98	Aug	0.82	Aug	-0.025	0.48
THD	Trinidad Head, California	40.0	-124.2	AGAGE	N <sub>2</sub> O	Oct 95	Sep	0.32	Jun	-0.019	0.48
THD				AGAGE	CFC-12	Oct 95	Aug	0.61 <sup>b</sup>	Aug	-0.047 <sup>b</sup>	<b>0.79</b>
CGO	Cape Grim, Tasmania	-40.7	144.7	AGAGE	N <sub>2</sub> O	Aug 93	May	0.44	Feb	-0.030	<b>0.86</b>
CGO				AGAGE	CFC-12	Aug 93	Apr	0.44 <sup>b</sup>	Feb	-0.025 <sup>b</sup>	<b>0.65</b>
CGO				N/CCGG	N <sub>2</sub> O	Apr 97	Apr	0.76	Jan	-0.034	<b>0.77</b>
CGO				CSIRO	N <sub>2</sub> O	Aug 92	May	0.55	Mar	-0.016	0.41

## Abiotic and biogeochemical signals

C. D. Nevison et al.

Title Page

Abstract

Introduction

Conclusions

References

Tables

Figures

◀

▶

◀

▶

Back

Close

Full Screen / Esc

Printer-friendly Version

Interactive Discussion



Abiotic and  
biogeochemical  
signals

C. D. Nevison et al.

Title Page

Abstract

Introduction

Conclusions

References

Tables

Figures

◀

▶

◀

▶

Back

Close

Full Screen / Esc

Printer-friendly Version

Interactive Discussion



Table 1. Continued.

Site	Name	Latitude	Longitude	Network <sup>a</sup>	Species	Starting date	Mean seasonal cycle		Correlation with stratospheric temperature		
							Month of minimum	Amplitude (ppb)	Month of best anti-correlation	Slope ppb K <sup>-1</sup>	<i>R</i>
CRZ	Crozet Island	-46.4	51.8	N/CCGG	N <sub>2</sub> O	Mar 97	Apr	0.72	Feb	-0.039	<b>0.68</b>
TDF	Tierra del Fuego	-54.5	-68.5	N/CCGG	N <sub>2</sub> O	Jun 97	May	0.78	Feb	-0.038	<b>0.77</b>
MQA	Macquarie Island	-54.5	159.0	CSIRO	N <sub>2</sub> O	Mar 92	May	0.56	May	-0.068	<b>0.75</b>
PSA	Palmer Station	-64.9	-64.0	N/CCGG	N <sub>2</sub> O	Apr 97	May	0.86	Mar	-0.027	<b>0.73</b>
CYA	Casey Station	-66.3	110.5	CSIRO	N <sub>2</sub> O	Nov 96	May	0.67	Apr	-0.023	0.55
MAA	Mawson	-67.6	62.9	CSIRO	N <sub>2</sub> O	Mar 92	May	0.43	Mar	-0.019	0.31
SYO	Syowa	-69.0	39.6	N/CCGG	N <sub>2</sub> O	Dec 95	Jun	0.80	Jan	-0.032	<b>0.67</b>
HBA	Halley Bay	-75.6	-26.4	N/CCGG	N <sub>2</sub> O	Feb 96	Apr	0.81	Mar	-0.025	<b>0.62</b>
SPO	South Pole	-90.0	-26.5	N/CCGG	N <sub>2</sub> O	Jan 97	May	0.75	Mar	-0.021	<b>0.48</b>
SPO				CSIRO	N <sub>2</sub> O	Jan 92	May	0.65	Mar	-0.018	0.39
SPO				N/CATS	N <sub>2</sub> O	Feb 98	May	0.53	Feb	-0.011	0.46
SPO				N/CATS	CFC-12	Mar 98	Apr	0.57 <sup>b</sup>	Feb	-0.044 <sup>b</sup>	0.49

<sup>a</sup> NOAA/CCGG, NOAA/HATS and NOAA/CATS abbreviated as N/CCGG, N/HATS and N/CATS;

<sup>b</sup> CFC-12 slopes and mean seasonal amplitudes are normalized to N<sub>2</sub>O units by multiplying by the ratio of the mean tropospheric mixing ratios  $x(\text{N}_2\text{O})/x(\text{CFC-12})$ , where  $x(\text{N}_2\text{O})$  is in ppb and  $x(\text{CFC-12})$  is in ppt.

**Abiotic and  
biogeochemical  
signals**

C. D. Nevison et al.

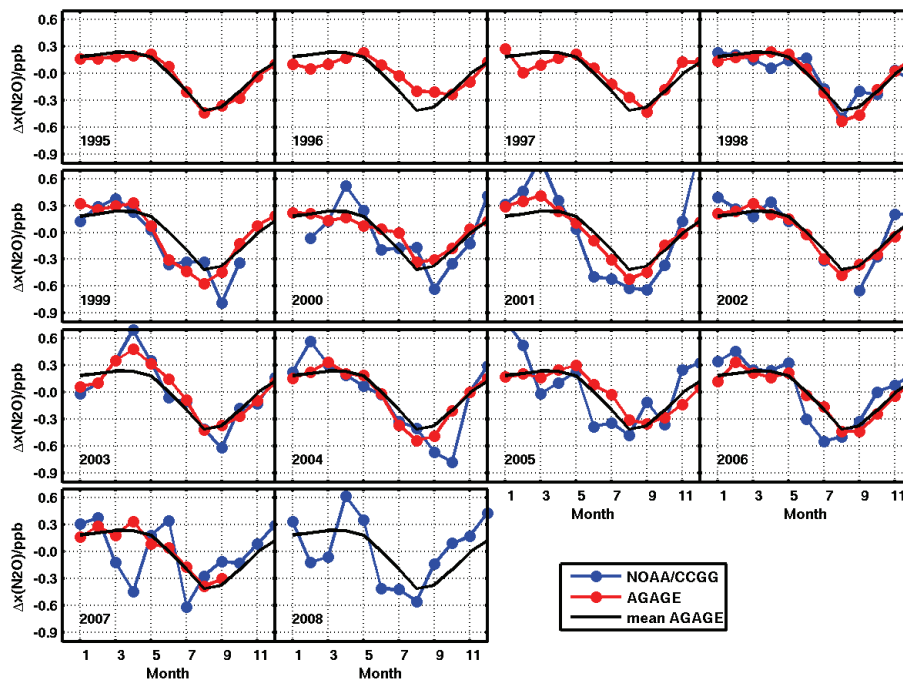


**Fig. 1a.** Monthly mean detrended  $\text{N}_2\text{O}$  residuals from AGAGE and NOAA/CCGG networks at Mace Head, Ireland.

Title Page

Abstract

Introduction

Conclusions

References

Tables

Figures

◀

▶

◀

▶

Back

Close

Full Screen / Esc

Printer-friendly Version

Interactive Discussion



Abiotic and  
biogeochemical  
signals

C. D. Nevison et al.

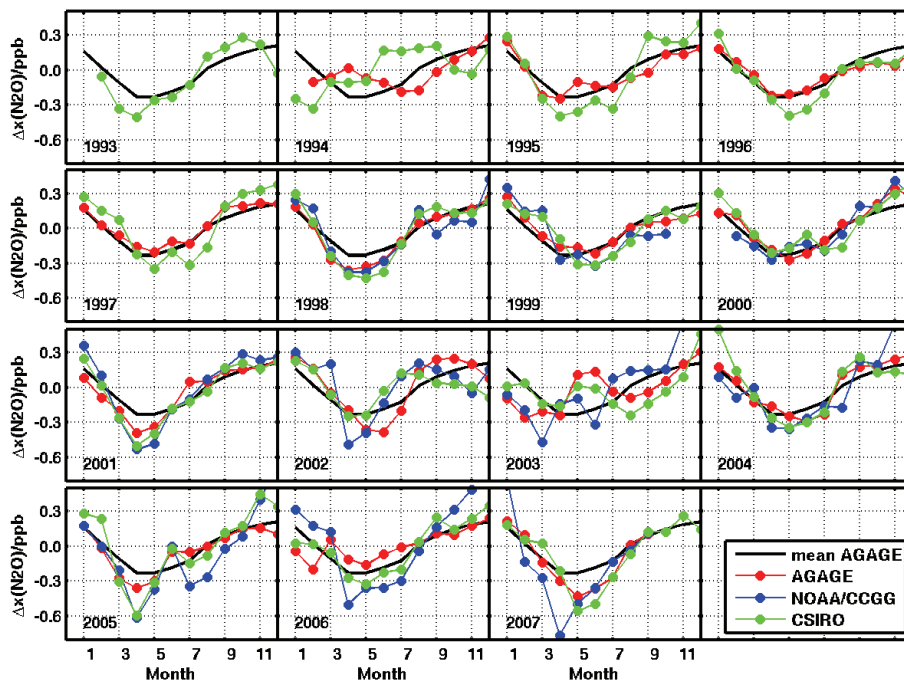


**Fig. 1b.** Monthly mean detrended  $N_2O$  residuals from AGAGE, NOAA/CCGG and CSIRO networks at Cape Grim, Tasmania.

Title Page

Abstract

Introduction

Conclusions

References

Tables

Figures

◀

▶

◀

▶

Back

Close

Full Screen / Esc

Printer-friendly Version

Interactive Discussion



**Abiotic and  
biogeochemical  
signals**

C. D. Nevison et al.

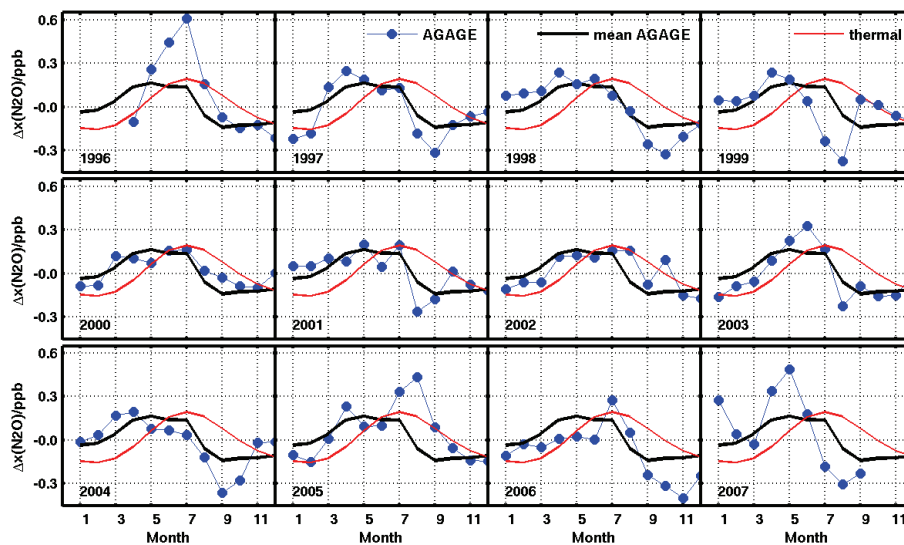


**Fig. 2.** Monthly mean detrended AGAGE N<sub>2</sub>O residuals at Trinidad Head, California. The “mean” annual cycle in observed N<sub>2</sub>O and estimated mean annual thermal N<sub>2</sub>O cycle associated with oceanic ingassing and outgassing are superimposed on each year’s observed cycle.

Title Page

Abstract

Introduction

Conclusions

References

Tables

Figures

◀

▶

◀

▶

Back

Close

Full Screen / Esc

Printer-friendly Version

Interactive Discussion



Abiotic and  
biogeochemical  
signals

C. D. Nevison et al.

Title Page

Abstract

Introduction

Conclusions

References

Tables

Figures

◀

▶

◀

▶

Back

Close

Full Screen / Esc

Printer-friendly Version

Interactive Discussion

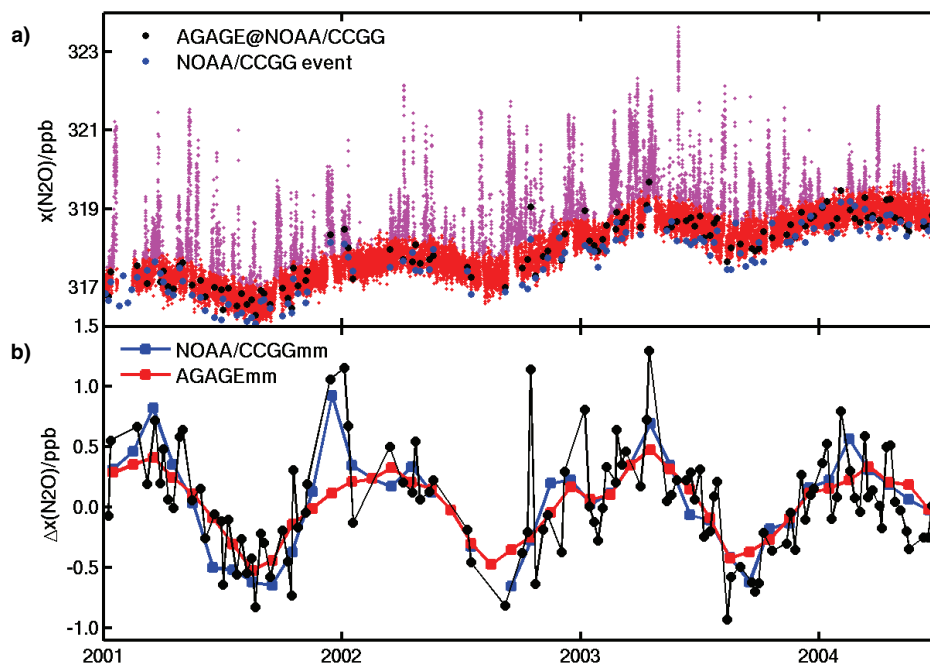


**Fig. 3.** (a)  $\text{N}_2\text{O}$  data at Mace Head, Ireland from January 2001–June 2004. Warm colors show complete AGAGE in situ data. Magenta indicates data tagged as pollution events. Blue dots are NOAA/CCGG event (i.e., weekly flask) data. Black circles are AGAGE data subsampled at the time of NOAA/CCGG flask collection. (b) AGAGE data subsampled at the time of NOAA/CCGG flask collection. Solid squares show the monthly mean data for AGAGE and NOAA/CCGG. All data have been detrended with a 12-month centered running mean of their respective networks.

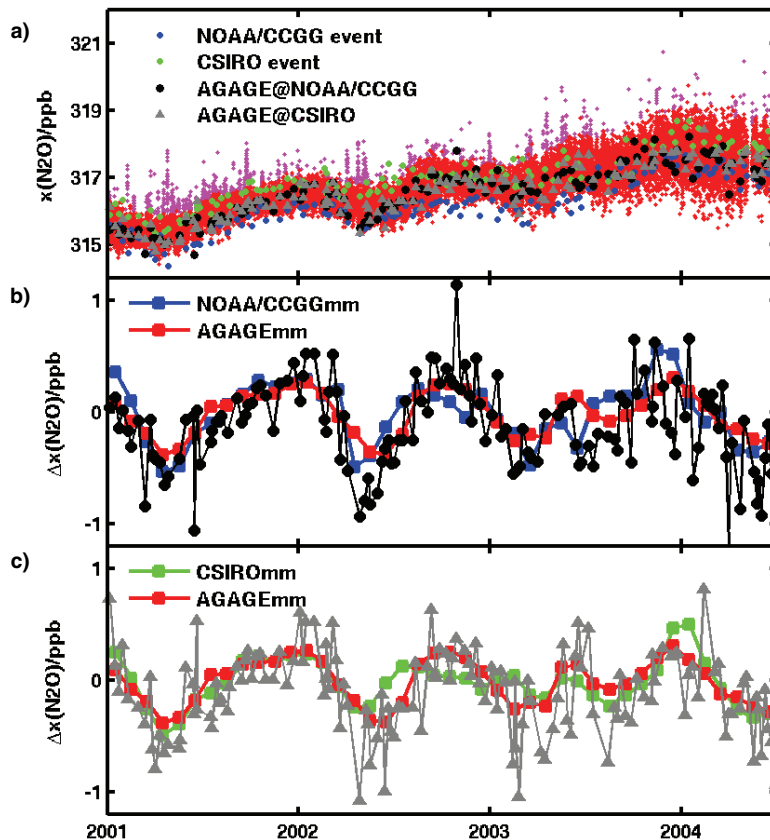


**Fig. 4.** (a) Same as Fig. 3a but for Cape Grim, Tasmania. Green dots are CSIRO event data. Gray triangles are AGAGE data subsampled at the time of CSIRO flask collection. (b) AGAGE data subsampled at NOAA/CCGG flask times compared to AGAGE and NOAA/CCGG monthly means. (c) AGAGE data subsampled at CSIRO flask times compared to AGAGE and CSIRO monthly means. All data in (b) and (c) have been detrended.

**Abiotic and biogeochemical signals**

C. D. Nevison et al.

Title Page

Abstract Introduction

Conclusions References

Tables Figures

◀ ▶

◀ ▶

Back Close

Full Screen / Esc

Printer-friendly Version

Interactive Discussion



**Abiotic and biogeochemical signals**

C. D. Nevison et al.

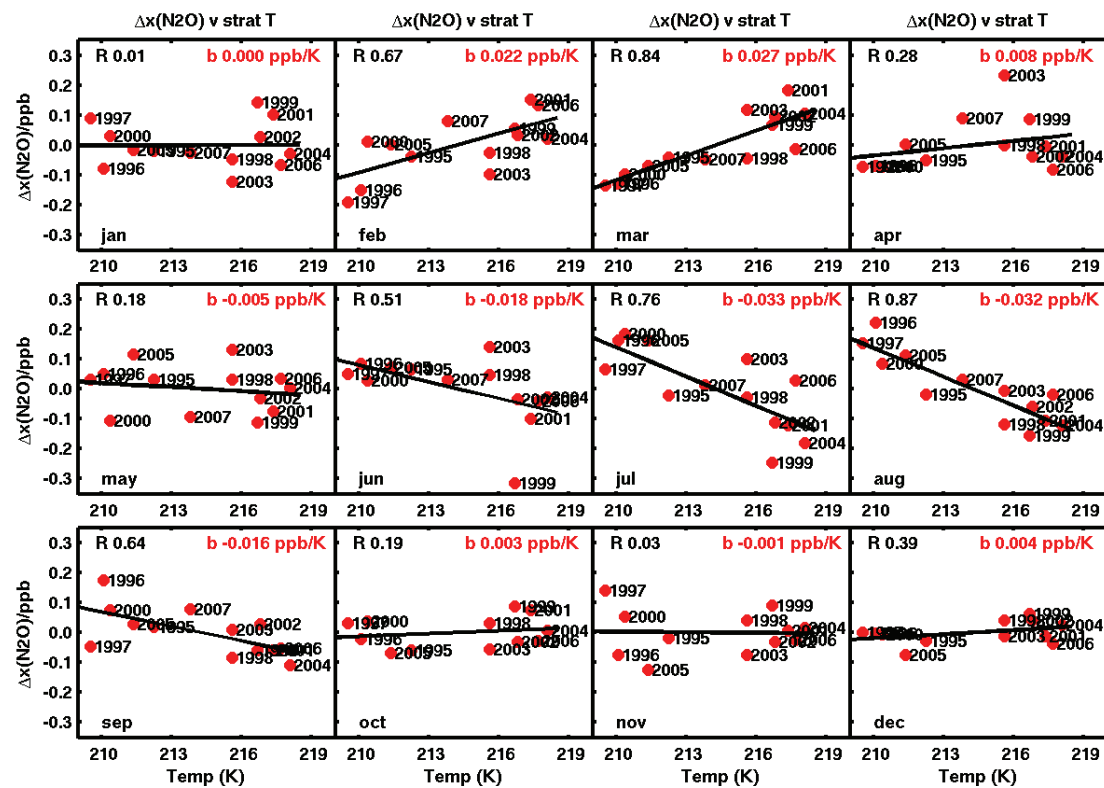


**Fig. 5.** Detrended AGAGE N<sub>2</sub>O data at Mace Head, Ireland (from Fig. 1a), sorted by month and plotted vs. mean polar (60–90° N) winter (January–March) lower stratospheric (100 hPa) temperature from NCEP reanalysis data. The mean of the detrended N<sub>2</sub>O data for each month is subtracted to permit all months to be plotted with the same y-axis scale. The Pearson's correlation coefficient *R* and the slope *b* of each linear regression are shown.

Title Page

Abstract Introduction

Conclusions References

Tables Figures

◀ ▶

◀ ▶

Back Close

Full Screen / Esc

Printer-friendly Version

Interactive Discussion



Abiotic and  
biogeochemical  
signals

C. D. Nevison et al.

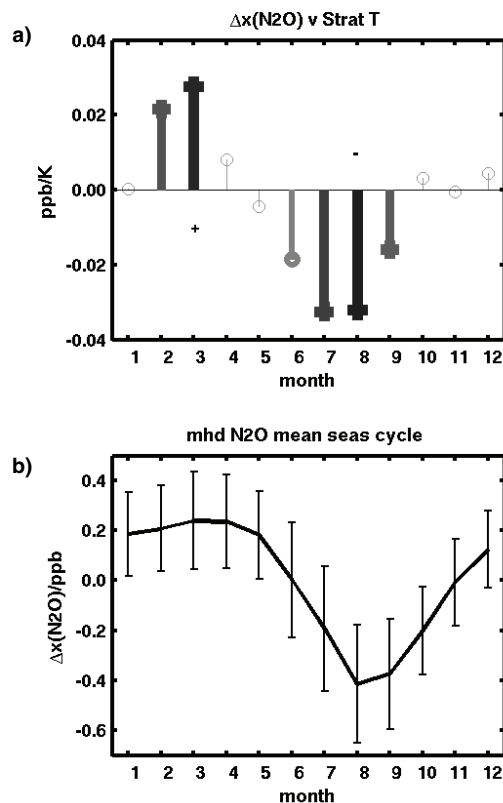


**Fig. 6.** (a) Stem plot summarizing the correlation slopes between AGAGE detrended N<sub>2</sub>O monthly means at Mace Head and northern polar winter lower stratospheric temperature from Fig. 5. Heavy lines indicate statistically significant correlations. The darker the line, the higher the *R* value. Negative slopes in July–September indicate deeper minima at warmer stratospheric temperature, (b) “mean” seasonal cycle at Mace Head for AGAGE N<sub>2</sub>O, with error bars showing the standard deviation for each month.

Title Page

Abstract

Introduction

Conclusions

References

Tables

Figures

◀

▶

◀

▶

Back

Close

Full Screen / Esc

Printer-friendly Version

Interactive Discussion



Abiotic and  
biogeochemical  
signals

C. D. Nevison et al.

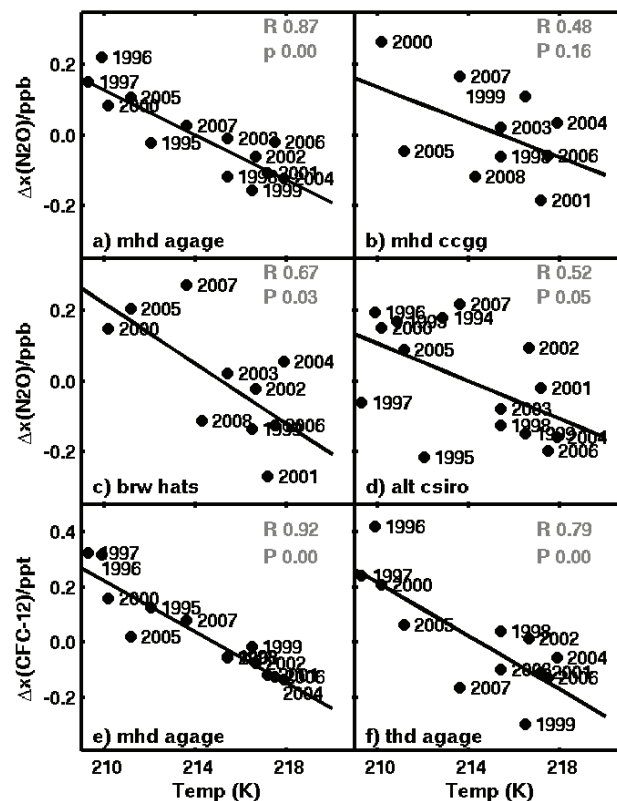


**Fig. 7.** Detrended  $\text{N}_2\text{O}$  residuals at the minimum month in the mean annual cycle (September for Alert, August for the other sites) vs. polar winter lower stratospheric temperature,  $\text{N}_2\text{O}$  (a–d) and CFC-12 (e, f) data are from AGAGE, NOAA/HATS, NOAA/CCGG or CSIRO monitoring sites as indicated on the panels. The Pearson's correlation coefficient  $R$  and the  $p$  value based on a Student's  $t$  distribution for each linear regression are shown, where a value of  $p \leq 0.05$  is statistically significant (Sokal and Rohlf, 1981).

Title Page

Abstract

Introduction

Conclusions

References

Tables

Figures

◀

▶

◀

▶

Back

Close

Full Screen / Esc

Printer-friendly Version

Interactive Discussion



## Abiotic and biogeochemical signals

C. D. Nevison et al.

Title Page

Abstract

Introduction

Conclusions

References

Tables

Figures

◀

▶

◀

▶

Back

Close

Full Screen / Esc

Printer-friendly Version

Interactive Discussion

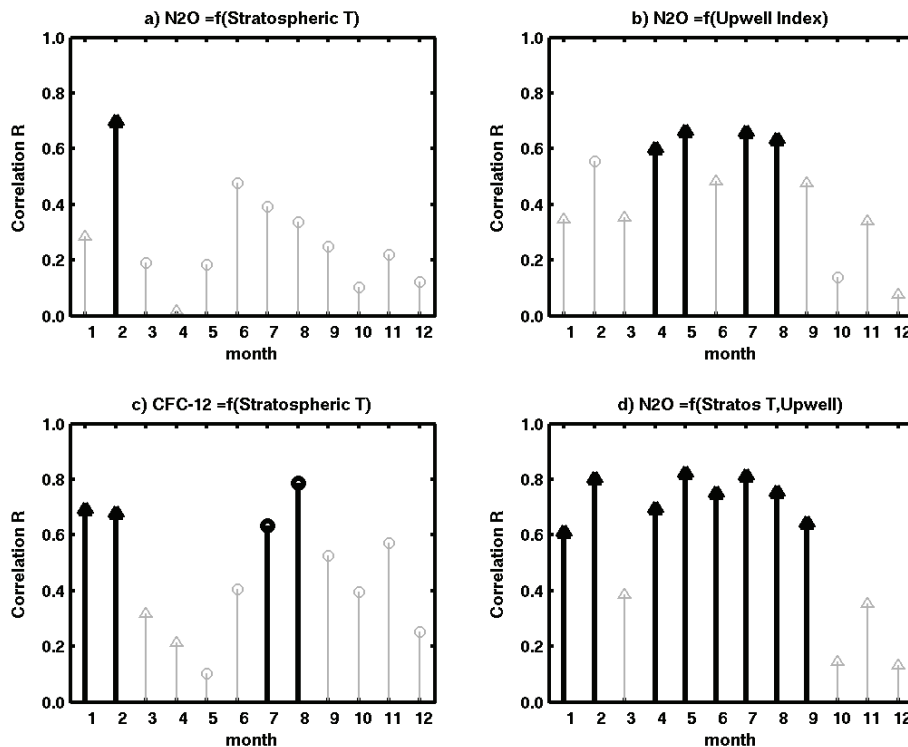


**Fig. 8.** Stem plots summarizing the linear regression slopes for detrended AGAGE  $N_2O$  or CFC-12 monthly means at Trinidad Head vs. polar winter lower stratospheric temperature and/or the NOAA PFEL upwelling index for the Oregon coast at  $45^\circ N$ . Heavy black lines indicate statistically significant correlations. Triangles indicate a positive correlation, circles indicate a negative correlation (e.g., in panel **c**, warmer stratospheric temperatures are correlated to more negative CFC-12 values in July–August, i.e., deeper seasonal minima). **(a)**  $N_2O$  vs. stratospheric temperature, **(b)**  $N_2O$  vs. upwelling index, **(c)** CFC-12 vs. stratospheric temperature, **(d)** multivariate regression of  $N_2O$  vs. stratospheric temperature and upwelling index.

Abiotic and  
biogeochemical  
signals

C. D. Nevison et al.

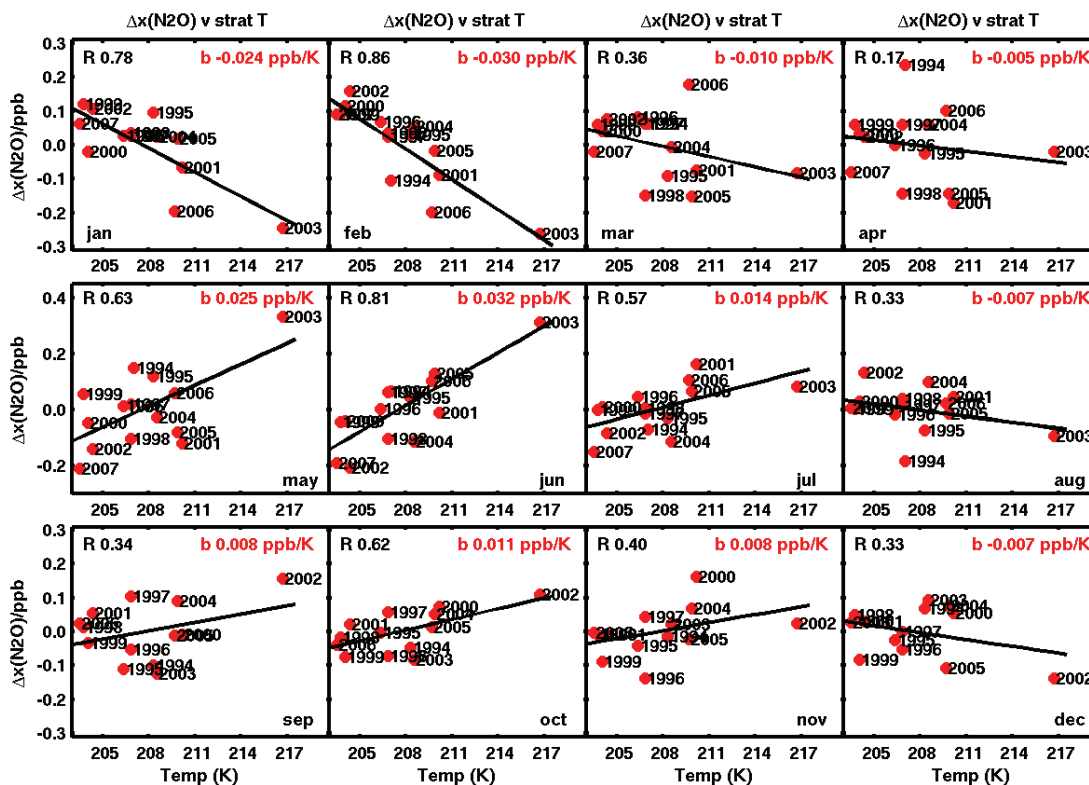


**Fig. 9.** Detrended AGAGE N<sub>2</sub>O data at Cape Grim, Tasmania (from Fig. 1b), sorted by month and plotted vs. mean polar (60–90° S) winter–spring (September–November) lower stratospheric (100 hPa) temperature from NCEP reanalysis data. The mean of the detrended N<sub>2</sub>O data for each month is subtracted to permit all months to be plotted with the same y-axis scale. The Pearson's correlation coefficient  $R$  and the slope  $b$  of each linear regression are shown. Note that the year labels correspond to the year of the detrended N<sub>2</sub>O monthly means, which for January–August are plotted against the previous year's late winter–spring (September–November) stratospheric temperature, when cold air is still generally trapped in the polar vortex. A sudden stratospheric warming occurred in September 2002, leading to anomalously warm polar temperatures in the spring lower stratosphere (Glatthor et al., 2005).

Title Page

Abstract

Introduction

Conclusions

References

Tables

Figures

◀

▶

◀

▶

Back

Close

Full Screen / Esc

Printer-friendly Version

Interactive Discussion



Abiotic and  
biogeochemical  
signals

C. D. Nevison et al.

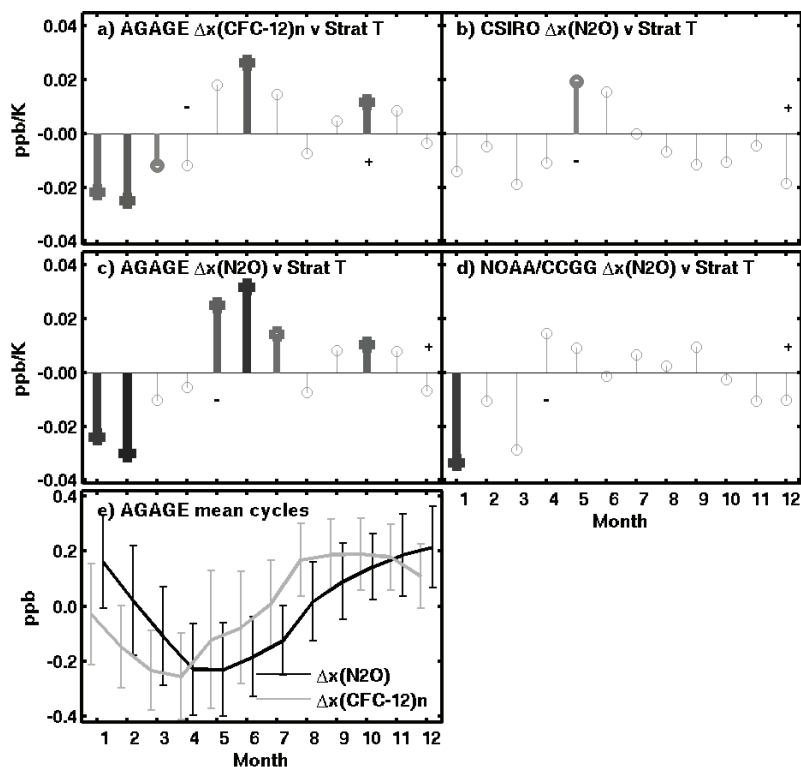


**Fig. 10.** Stem plots summarizing the linear regression slopes for detrended N<sub>2</sub>O or CFC-12 monthly means at Cape Grim vs. mean southern polar winter–spring lower stratospheric temperature. Heavy lines indicate statistically significant correlations. The darker the line, the higher the  $R$  value: **(a)** AGAGE CFC-12, normalized by  $[x(\text{N}_2\text{O})/\text{ppb}]/[x(\text{CFC-12})/\text{ppt}]$  and expressed in ppb units, **(b)** CSIRO N<sub>2</sub>O, **(c)** AGAGE N<sub>2</sub>O, **(d)** NOAA/CCGG N<sub>2</sub>O, **(e)** mean seasonal cycle for AGAGE N<sub>2</sub>O and normalized CFC-12, with error bars showing the standard deviation for each month.

Title Page

Abstract

Introduction

Conclusions

References

Tables

Figures

◀

▶

◀

▶

Back

Close

Full Screen / Esc

Printer-friendly Version

Interactive Discussion



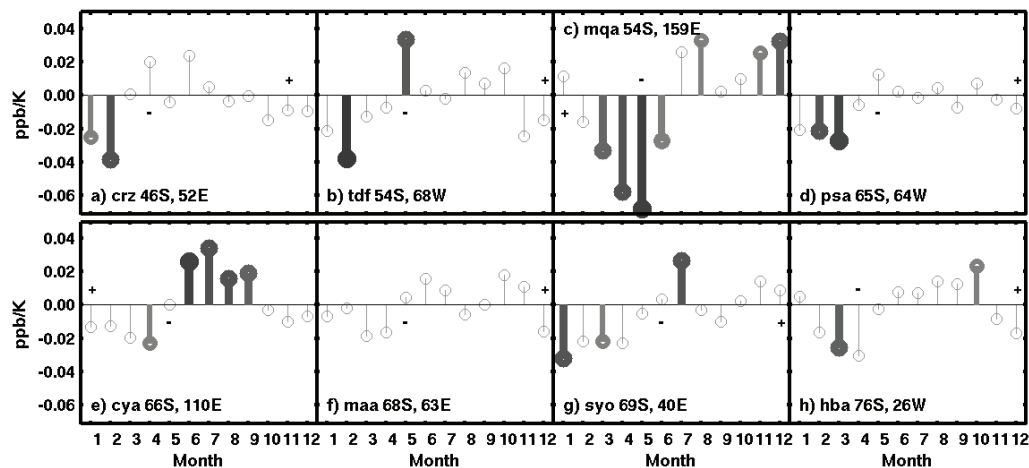


**Fig. 11.** Stem plots summarizing the linear regression slopes for detrended  $\text{N}_2\text{O}$  monthly means at 8 different Southern Hemisphere sites spanning 3 monitoring networks vs. mean southern polar winter–spring lower stratospheric temperature. Heavy lines indicate statistically significant correlations at the 5% confidence level, with darker lines, signifying higher  $R$  values. Medium grey lines with open circles indicate marginally significant correlations at 10% confidence level: **(a)** Crozet Island (NOAA/CCGG), **(b)** Tierra del Fuego (NOAA/CCGG), **(c)** Macquarie Island (CSIRO), **(d)** Palmer Station (NOAA/CCGG), **(e)** Casey Station (CSIRO), **(f)** Mawson (CSIRO), **(g)** Syowa (NOAA/CCGG), **(h)** Halley Bay (NOAA/CCGG).

## Abiotic and biogeochemical signals

C. D. Nevison et al.

Title Page

Abstract

Introduction

Conclusions

References

Tables

Figures

◀

▶

◀

▶

Back

Close

Full Screen / Esc

Printer-friendly Version

Interactive Discussion



## Abiotic and biogeochemical signals

C. D. Nevison et al.

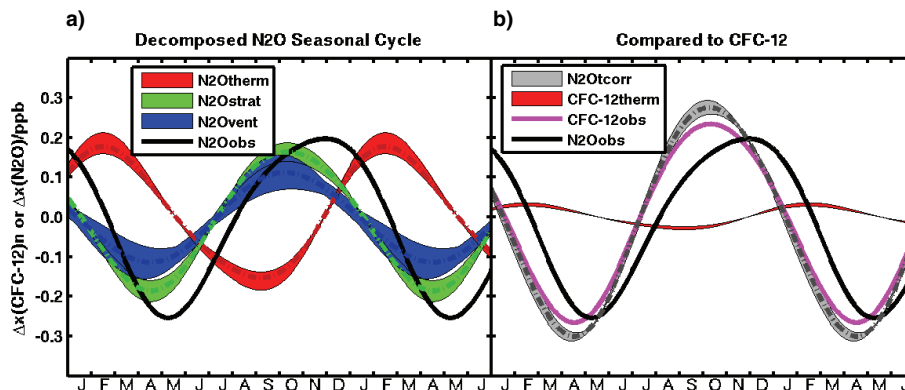


**Fig. 12.** (a) Decomposition of N<sub>2</sub>O seasonal cycle at Cape Grim based on methodology described in Nevison et al. (2005). Envelopes show estimated uncertainty in stratospheric and thermal signals, with the biological oceanic ventilation signal derived as a residual of observed N<sub>2</sub>O minus the thermal and stratospheric terms. Figure uses smoothed, idealized curves. (b) Comparison of observed CFC-12 seasonal cycle at Cape Grim to observed N<sub>2</sub>O cycle, before and after correcting N<sub>2</sub>O for the thermal signal from (a). The corresponding thermal signal in CFC-12 is small (red envelope) and does not substantially change the observed CFC-12 seasonal cycle. The observed and thermal CFC-12 curves are shown in ppb units, after being normalized by  $[x(\text{N}_2\text{O})/\text{ppb}]/[x(\text{CFC-12})/\text{ppt}]$ .

Title Page

Abstract

Introduction

Conclusions

References

Tables

Figures

◀

▶

◀

▶

Back

Close

Full Screen / Esc

Printer-friendly Version

Interactive Discussion